Spatial Statistics xxx (xxxx) xxx

Contents lists available at ScienceDirect

Spatial Statistics

journal homepage: www.elsevier.com/locate/spasta

Concept-driven extraction of the Antarctic marginal sea ice zone from remote sensing image time series

Xi Zhao [a], Yue Liu [b,*], Xiaoping Pang [b], Qing Ji [b], Alfred Stein [c], Xiao Cheng [a], Ying Chen [b]

[a] School of Geospatial Engineering and Science, Sun Yat-Sen University & Southern Marine Science and Engineering Guangdong Laboratory(Zhuhai), Zhuhai 519000, China
[b] Chinese Antarctic Center of Surveying and Mapping, Wuhan University, Wuhan 430079, China
[c] Faculty of Geo-Information Science and Earth Observation (ITC), University of Twente, The Netherlands

ARTICLE INFO

Article history:
Received 10 November 2021
Received in revised form 23 December 2021
Accepted 23 December 2021
Available online xxxx

Keywords:
Marginal ice zone
Fuzzy inference system
Membership
Antarctic
Remote sensing

ABSTRACT

Sea ice plays a significant role in global climate change. Marginal ice zone (MIZ) is defined as the transition zone between open ocean and pack ice where intensive air–ice–ocean–wave interactions between the ocean and the atmosphere occur. This definition of MIZ is rather vague, which affects its mapping. Previous data-driven methods extracted MIZ from single source data and conveniently used a single classification threshold. In this study, we propose to apply a concept-driven top down extraction method. We use a fuzzy inference system (FIS) to integrate multiple ice properties based upon the MIZ definition, and use membership functions to quantify the uncertainty of the threshold for several ice characteristics. This concept-driven method is applied to mapping the Antarctic MIZ between 2010 and 2021. Results show that a FIS successfully combines the ice concentration and ice thickness, while it allowed us to map the MIZ as objects with vague boundaries, thus well-presenting its indeterminate nature in space.

* Corresponding author.
E-mail addresses: zhaoxi6@mail.sysu.edu.cn (X. Zhao), yue.liu@whu.edu.cn, pxp@whu.edu.cn (Y. Liu), pxp@whu.edu.cn (X. Pang), jiqing@whu.edu.cn (Q. Ji), a.stein@utwente.nl (A. Stein), chengxiao9@mail.sysu.edu.cn (X. Cheng), chen_ying@whu.edu.cn (Y. Chen).

https://doi.org/10.1016/j.spasta.2021.100578
2211-6753/

Please cite this article as: X. Zhao, Y. Liu, X. Pang et al., Concept-driven extraction of the Antarctic marginal sea ice zone from remote sensing image time series. Spatial Statistics (2022) 100578, https://doi.org/10.1016/j.spasta.2021.100578.

1. Introduction

Sea ice is frozen from seawater and floats on the ocean's surface. Since sea ice covers approximately 12% of the world's oceans, its changes in the polar regions play an important role in the global climate system. Sea ice undergoes a large yearly cycling in surface extent. In winter, as temperature is decreasing, large amounts of sea ice form and act as insulators between ocean and the atmosphere. Snow cover and ice packs with high albedo reflect much of the solar radiation and keep the underlying ocean warm. In summer, as sea ice is melting, the thinner ice pack and exposed water area with less reflectivity absorb solar energy, which further accelerates the retreat process. In contrast to the rapidly declining sea ice in the Arctic, the extent of Antarctic sea ice shows a slightly increasing trend but also shows accelerated fluctuation and large regional variability (Zhao et al., 2016). The sea ice extent in the Antarctic region varies between approximately 3 million km^2 in February to approximately 18 million km^2 in September (Shokr and Sinha, 2015).

Due to the joint action of winds and currents, sea ice is highly dynamic and shows a changing composition in its several forms of ice types. Waves penetrate several kilometers into the ice area and break the large ice pack into smaller ice floes. This creates a marginal ice zone (MIZ) at the fringe of the denser ice region. This resulted into the definition of the MIZ as "… the zone at the edge of the pack ice whose width is the lateral distance over which the penetration of waves can fracture the ice, thereby changing the morphology of the floes" (Weeks, 2010). Another definition of the MIZ, from a geographical perspective, is a transition region from open water to pack ice with changing concentration, thickness, and ice floe sizes and shapes (Lee et al., 2012). To facilitate the spatial analysis, the MIZ is then defined as extending from the outer sea ice–open-ocean boundary to the boundary of the consolidated pack ice (Strong, 2012; Stroeve et al., 2016).

The MIZ provides a physical buffer that protects the more consolidated inner pack from the effects of ocean waves (e.g., Squire (2007)). The MIZ with smaller floes is more susceptible to melting, since water areas between floes can absorb more solar radiation and accelerate the ice decay. Intensive exchanges of heat and moisture between ocean and atmosphere occur in the MIZ, which makes this zone a highly suited observation area to study air–ice–ocean–wave interactions. In the MIZ, the upper layer water produces optimal conditions for phytoplankton production and krill abundance, on which fish, seabirds and marine mammals rely for their survival. Mapping of the MIZ extent and its spatial–temporal variability is therefore a basic and vital step for understanding the complex physical interactions and habitat functionality.

The importance of the MIZ has motivated various estimates of its extent as based upon satellite remote sensing images. Several studies mapping the MIZ based upon sea ice concentrations were generated using passive microwave satellite data (Strong, 2012; Strong and Rigor, 2013; Williams et al., 2014; Stroeve et al., 2016; Liu et al., 2021). They defined the MIZ as the extent from the outer sea ice–open-ocean boundary to the boundary of the consolidated pack ice. These boundaries are where the Sea Ice Concentration (SIC) equals 0.15, being the conventional ice edge, and 0.80, being the edge with close ice, respectively (Comiso, 2006; WMO, 2014). Once the boundaries of the MIZ have been identified, the MIZ width could be obtained as well its mathematical properties (Strong, 2012; Strong et al., 2017). In succeeding applications, Strong and Rigor (2013) and Stroeve et al. (2016) revealed the MIZ spatial–temporal variability in the Arctic and Antarctic. Besides, Stroeve et al. (2016) tested two popular ice concentration retrieval algorithms, and found that the significance of trends at least for some part depend upon the ice concentration input data. The above-mentioned MIZ mapping methods are developed based upon a single data source and from the perspective of data use convenience, and hence we call them data-driven methods.

The MIZ is regarded as a transition area between the open ocean and the consolidated pack ice, and this human defined concept corresponds to a vague object in the real world. Ideally, when mapping, one first has a concept definition, and then observes several physical properties such as in this case for instance ice concentration, thickness, surface temperature, floe size distribution and drift velocity. One then matches these observed properties with the concept definition. This concept-driven method can realize a top-down MIZ mapping process, which is different from a data-driven method starting from the data. Since the concept of MIZ relies on several sea ice properties that need to be integrated, this study proposes a fuzzy inference system (FIS) to build a framework

that organizes multiple properties and build the relationships with the defining concept. As an initial exploration, we focus on two main sea ice properties: sea ice concentration and sea ice thickness. Other properties can be involved when observation data are prepared.

2. MIZ definition and FIS construction

2.1. MIZ definition

In this study, we follow the definition of MIZ by Lee et al. (2012). It is a region with two boundaries: a lower boundary between MIZ and open water, and an upper boundary between MIZ and pack ice. Since there is no such physical boundary in the real word, we need to extract the sudden change places and treat them as the boundaries. To further interpret this concept, we need to address two issues:

(1) What is exactly changing, as several properties such as ice concentration and thickness are recorded as spatial variables. These spatial variables can be analyzed, for instance by integrating them into a single representative variable as a proxy to the MIZ boundary.

(2) How to describe the sudden change, as the spatial properties are recorded by two dimensional variables. For each variable, the gradient that describes the change in neighborhood can then be quantified. For instance, a large gradient indicates sudden changes and can be extracted as a boundary line.

In this study we will use fuzzy methods. We first give a brief introduction to a Fuzzy Inference System (FIS) that was used as an integration method. We will also provide information from remote sensing datasets used as FIS input and introduce methods for obtaining the gradient.

2.2. FIS

Fuzzy inference interprets the values in the input and, based upon a set of rules and fuzzy logic, assigns values to the output, usually as a membership degree (Yuan et al., 2011). An FIS uses fuzzy logic theory as the core of the methodology, which can realize complex nonlinear mapping (Li et al., 2002). An FIS consists of four parts: fuzzification, fuzzy rules, fuzzy logic operators, and defuzzification (Fig. 2). Fuzzification is the process of transforming the crisp input values to values between zero and one, using a set of input membership functions. These input membership functions represent fuzzy concepts and are used to describe the indeterminate boundary thresholds in this study. Fuzzy rules are a collection of linguistic statements that describe how an FIS should make a decision regarding classifying an input or controlling an output (Zadeh, 1975; Manton et al., 1994). Fuzzy rules are composed of fuzzy expressions that are connected by fuzzy logical operators, written in the if-then form:

$$R^i\text{: IF } x_1 \text{ is } A_1^i \text{ AND } x_2 \text{ is } A_2^i \text{ AND } \ldots x_n \text{ is } A_n^i \text{ THEN } y_s \text{ is } B^i$$

where $X = (x_1, x_2, \ldots, x_n)$ present the input and $Y = (y_1, y_2, \ldots, y_n)$ the output datasets, respectively.$A_1^i, A_2^i, \ldots, A_n^i$ and B^i present the membership functions in the ith rule. Except for intersection (AND), also union (OR) and complementation (NOT) are important logical operators that are commonly applied in building fuzzy relations. After aggregation, a fuzzy set exists for the output variable. In case a single crisp output is desired, several defuzzification methods such as taking the centroid, the mean, the maximum or a pre-defined alpha-cut can be applied.

2.3. Data

With the advantages of daylight- and weather-independent observations, SIC taken from passive microwave sensors have provided nearly complete and consistent records of sea-ice distribution for more than four decades Parkinson (2019). SIC datasets of used in this study were derived from long-term passive microwave data records that span several satellite missions. These include the Scanning Multichannel Microwave Radiometer (SMMR) on the Nimbus-7 satellite (October 1978 to August 1987), the Special Sensor Microwave Imager (SSM/I) sensors F8 (July 1987 to December

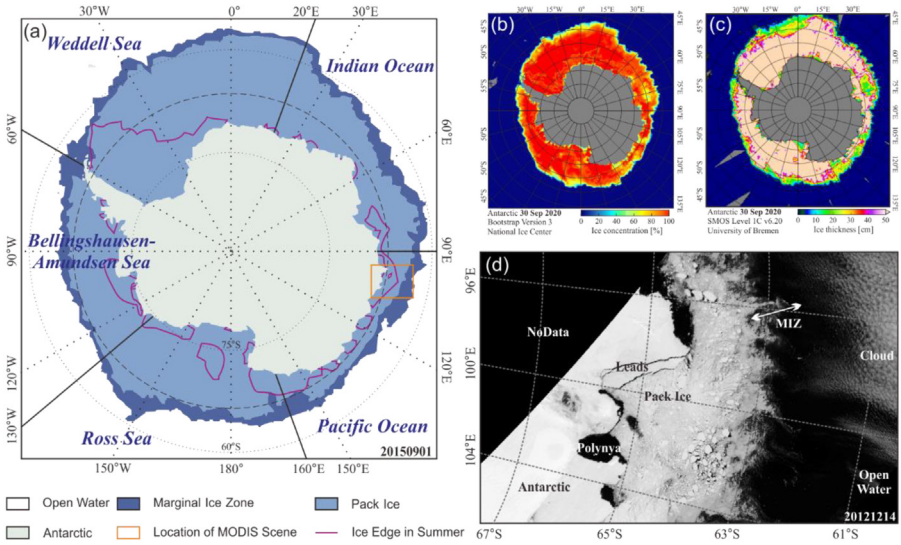

Fig. 1. Study area and data. (a) Marginal ice zone is on the periphery of sea ice region which surrounds Antarctic ice sheet, derived from data in winter at Sept. 1st 2015. (b) An example of ice concentration data. (c) An example of thin ice thickness data. (d) MIZ observed from MODIS image at 500 m resolution.

1991), F11 (December 1991 to September 1995) and F13 (May 1995 to December 2007), and the Special Sensor Microwave Imager/Sounder (SSMIS) sensor F17 (January 2007 to present), all on the Defense Meteorological Satellite Program's (DMSP) satellites. We obtained the SIC products processed using the Bootstrap algorithm which were published on the National Snow and Ice Data Center. The SIC products are gridded on an SSM/I polar stereographic grid at a 25 km spatial resolution, covering the south polar regions for the period from 1 January 1979 to 31 December 2020.

Thin sea ice thickness (SIT) is daily retrieved from observations of the L-band microwave sensor SMOS (Soil Moisture and Ocean Salinity) using an empirical method. We obtained the SIT products published by the University of Bremen at a 12.5 km spatial resolution (Huntemann et al., 2014). Since SIT retrieval methods are not yet able to generate reliable results during ice melting, we only used meaningful results from March to September from 2010 to 2020.

The SIC and SIT datasets were processed to be at the same projection and at a 12.5 km resolution (Fig. 1). Both daily datasets cover seven months (March to September) for eleven years (2010 to 2020). SIC values range from 0 to 100%, indicating the fraction of ice in the pixel, while SIT values range indicate thin ice thickness from 0 to 50 cm. Polynyas which have similar SIC and SIT range but are located near the coast were masked out during pre-processing. After the final MIZ extent was identified, post-processing was applied to fill holes, mask small icebergs and filter isolated small ice floes (Fig. 2).

3. Gradient and fuzzy membership function

Both SIC and SIT data are spatially continuous variables, reflecting the gradual boundaries between dense ice pack and MIZ, MIZ and open water. Previous studies adopted values of 15% and 80% as the SIC thresholds, and 0 and 20 cm as SIT thresholds when making a crisp classification. These thresholds, however, can shift slightly between datasets derived from different sensors or even by different retrieval algorithms. In this study we propose to use a gradient index to determine the threshold scene by scene, and to construct membership functions that present the variability of the thresholds.

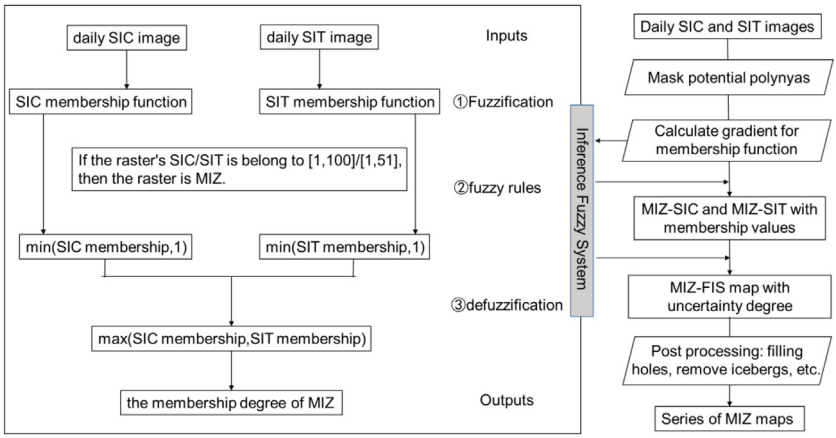

Fig. 2. Workflow chart of FIS and data processing.

3.1. Gradient calculation

A spatial classification commonly starts from the idea that differences between different classes are larger than those within the same class and that there is an obvious change across boundaries. To identify representative change values, we use the gradient index $G(k)$ that quantifies the degree of change at a single ice property (here: SIC or SIT). It is defined as (Zhang et al., 2018):

$$G\,(k) = \delta(k)/\varepsilon\,(k) \tag{1}$$

where $\varepsilon\,(k)$ is the total number of pixels with the ice property at value k, where k can be either SIC or SIT, and$\delta(k)$ is the number of times that the pixel values exceed the critical value (10% for SIC and 5 cm for SIT) as compared with the surrounding pixels in four directions. A large the gradient index $G\,(k)$ corresponds with a strong change at k.

With the increase of SIC or SIT, the gradient index in an MIZ region will first increase, then fluctuate slightly, and finally decrease, showing an overall gradual trend. Local maxima of $G\,(k)$ will correspond to the upper and lower thresholds of the MIZ region. To identify the local maxima, $\tau\,(k)$ describes the change slope of $G\,(k)$:

$$\tau\,(k) = \partial G(k)/\partial k, k \in [k_1, k_2] \tag{2}$$

where $[k_1, k_2]$ is a pre-defined range of the ice property. The k with $\max(\tau\,(k))$ is identified as a threshold. In this study, we constrained the lower and upper threshold of SIC with $k_{SIC\_lower} \in [1, 30]$, SIC $k_{SIC\_upper} \in [71, 100]$, respectively, and the lower and upper threshold of SIT with $k_{SIT\_lower} \in [1, 6]$, $k_{SIT\_upper} \in [10, 30]$, respectively.

Fig. 3(a) and Fig. (c) show the upper and lower thresholds extracted from every single SIC and SIT scene. Our first impression is that the values of four thresholds all have continual oscillations. Two lines represent the SIC thresholds in the upper panel of Fig. 3(a) and show a larger fluctuation than those in the lower panel (c) representing the SIT thresholds. Among these, the lower SIC thresholds show the biggest variation. This indicates that MIZ bounders tend to have more consistent SIT values than SIC values. The histograms summarizing the distribution of the thresholds in Fig. 3(b) and (d) show that the modes of SIT are equal to 5 cm and 22 cm, corresponding to the lower and upper thresholds respectively. As for the SIC, the mode at 79% presents the upper threshold, while the mode at 16%–17% represents the lower threshold. These values are consistent with the conventional usage of SIT and SIC thresholds, but give more information on their variability beyond the central values.

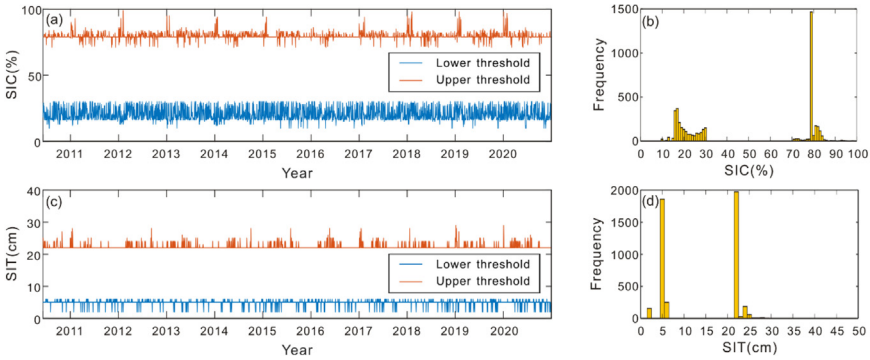

Fig. 3. Thresholds of ice concentration (a) and ice thickness (c) based upon the gradient of SIC and SIT on daily scenes; (b) histogram of SIC thresholds, (d) histogram of SIT thresholds.

3.2. Membership function

A membership function for a fuzzy set A on the universe of discourse X is defined as μ_A: X → [0, 1], where each element of X is mapped to a value between 0 and 1. This membership value quantifies the grade of membership of the element in X to the fuzzy set A. There are several methods for constructing membership function, including fuzzy statistics (Zadeh, 1978), binary comparison ranking (Wang et al., 2014) and expert investigation (Hong and Lee, 1996). In most cases, determination of the membership function is based on experiment or expert knowledge, or the function is fitted by graph line following a large number of survey data.

We obtain the expression of the membership function by fuzzy statistics. Its steps are as follows: first we select a domain U; second we select a fixed element u_0 in the U; third, an ordinary set A^* is a random realization of a fuzzy set A in U. Each determination of A^* is a definite division of the corresponding fuzzy concept A and each experiment should judge on whether u_0 belongs to A^*. After a series of n experiments, we obtain the membership value at u_0 as

$$u_A = sum(I(u_o \in A^*))/n \tag{3}$$

where $I(u_0 \in A^*)$ is the indicator function. By using Eq. (3), the membership frequencies of several fixed elements u_0 in the U can be determined, and the approximate shape of the membership function can be identified.

In this study, n equals the number of SIC maps and SIT maps, while every MIZ threshold interval extracted from a gradient map is an A^*. Fuzzy membership functions in Fig. 4 provide a graphical way of visualizing degree of membership of any SIC or SIT values in a given MIZ set. The x axis represents the universe of SIC and SIT properties, and the y axis represents the degree of membership in the [0, 1] interval. According to Fig. 4, when the SIC is below 10%, the membership degree is 0. If the SIC falls within the 10%–30% interval, the membership degree grows rapidly to 1, which forms the start of the support of MIZ set. SIC values between 30% and 71% were assigned a membership degree equal to 1, thus forming the core of the MIZ set. The membership degree gradually decreases to 0.93 at 79% SIC and then rapidly declines to 0.28 at 80%. With SIC increasing to 100%, the membership degree decreases to 0. The membership of SIT changes more sharply than that of SIC, with a core set between 6 and 21 cm, and narrower support sets. This suggests that the MIZ has more diverse SIC properties than SIT, and the membership functions are expected to delineate uncertainty hidden in concept definition and data processing.

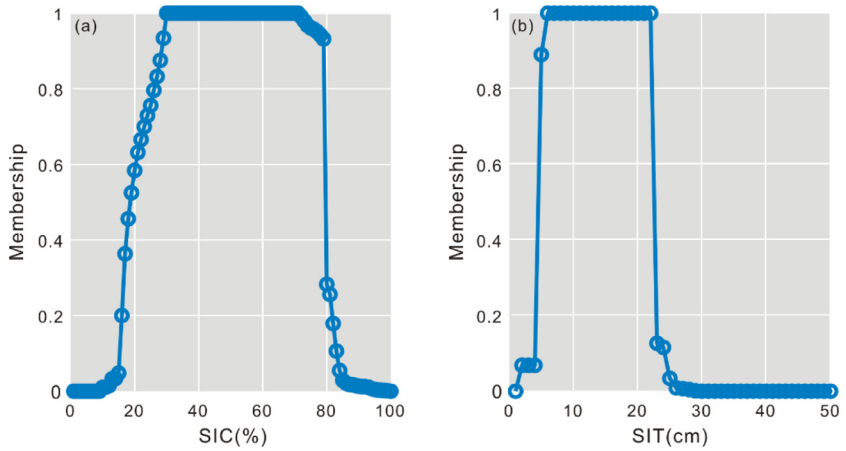

Fig. 4. Membership function graphs of (a) SIC and (b) SIT.

4. Spatial–temporal distribution of miz

4.1. Spatial distribution

Fig. 5(a) reveals that the MIZ located at the edge of sea ice extent, which is shaped as a narrow band. From March to September, as the sea ice area expands and the MIZ also moves northward, a larger total area and longer perimeter is visible. Instead of a crisp boundary, the MIZs are delineated by gradual change boundaries using membership degrees, from the perspective of ice concentration (MIZ-SIC in the first row), ice thickness (MIZ-SIT in the second row) and the integrated concept (MIZ-FIS in the third row). We observe that MIZ-SIC assigns a larger core area in red than MIZ-SIT, and that its extent has a higher similarity with MIZ-FIS. This confirms with what we noticed during fuzzy inference, i.e. most of the SIC with a larger membership value than SIT dominates the inference output. Besides, MIZ-SIC has a wider support area than MIZ-SIT, which is consistent with the characteristics of their membership functions in Fig. 4.

We selected MIZ maps on two days to enlarge some regions and show details on the difference. At April 14th, sea ice just starts to grow after surviving from the Antarctic summer, and the MIZ is located close to the coast. For regions A2, B2 and C2 in Fig. 5(c), MIZ-SIT shows a wider MIZ band than MIZ-SIC, where some thin ice was just frozen and classified as MIZ upon using SIT data. Such thin ice could form continuously in space and have a high SIC. Therefore, it was screened out by SIC data. Through FIS that combines both MIZ and SIT, such thin ice with a high SIC value was correctly classified as MIZ. At September 16th, when sea ice reaches its yearly maximum extent, the MIZ has a relatively wider extent and a more obvious support area. MIZ-SIC identified slightly larger extents than MIZ-SIT, with the difference corresponding to the thick ice area where waves penetrate that break ice into small pieces. This resulted into low SIC values but high SIT values. This condition was again successfully captured by the MIZ-FIS.

4.2. Temporal trend

Fig. 6 shows time series of the MIZ extent between 2011 and 2020. The shaded areas in Fig. 6(a) and (b) delineate the uncertain intervals of MIZ-SIC and MIZ-SIT that can be caused by threshold selection in MIZ extraction process. The thin solid lines represent the MIZ area with the membership value of 0.3. The position of the thin solid line in Fig. 6(a) is close to the upper half of the shaded area, whereas the thin solid line in Fig. 6(b) is close to the lower half of the shaded area. This reveals that MIZ-SIC has a large uncertain area with low membership values or in other words low confidence.

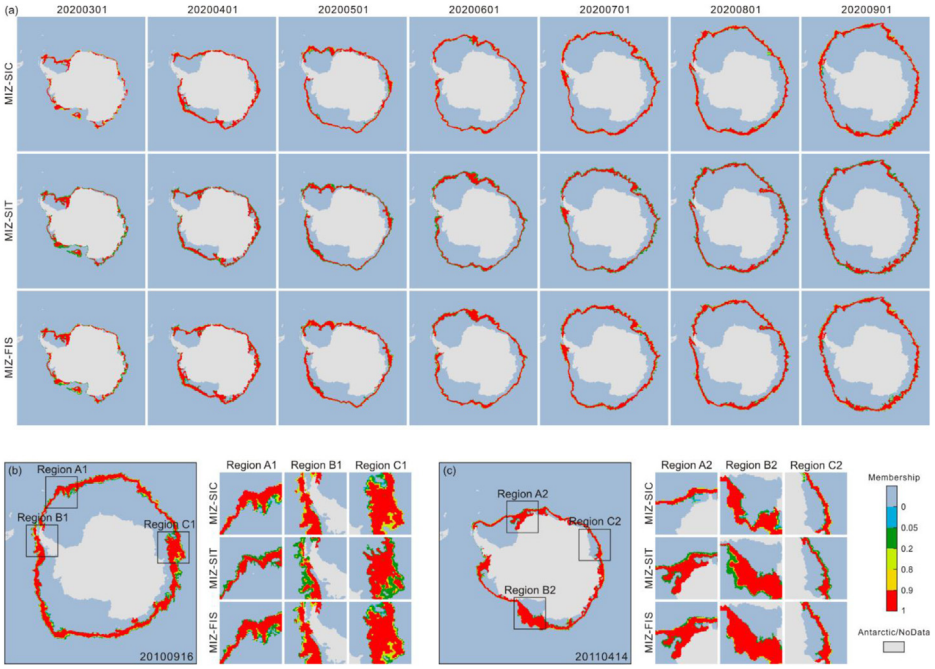

Fig. 5. Spatial distribution of Antarctic MIZ (a) MIZ extents generated by three methods: MIZ-SIC, MIZ-SIT, MIZ-FIS in different months, using the first day as an example. (b) MIZ map on September 16th 2010, three regions A1 to C1 were enlarged to show details. (c) MIZ map on April 14th 2011, three regions A2 to C2 were enlarged to show details.

In contrast, membership values of this part are larger, although MIZ-SIT also has uncertain parts, so the corresponding support area of MIZ-SIT is smaller. After integrating the concepts, MIZ-FIS gives a comprehensive result with the thin solid line in the middle of the uncertain interval. We used the membership value equal to 0.3 as the alpha-cut (the reason is discussed in Section 5) to obtain the MIZ extent derived from MIZ-SIC, MIZ-SIT and MIZ-FIS. Fig. 6(d) shows the three lines, displaying similar trends and fluctuations. Compared with MIZ-SIT, the line of MIZ-FIS is closer to MIZ-SIC, which indicates that ice concentration dominates the MIZ determination and thin ice thickness acts as supplementary information in most cases.

From the time series in Fig. 5(a) and Fig. 6(d), we observe that the MIZ area is smallest in March, with a minimum monthly average area value 2.01×10^6 km^2, accounting for 49.89% of the total sea ice area. The monthly average area grows continuously until September, reaching the maximum at value of 3.62×10^6 km^2, accounting for 18% of the total sea ice area. The time series data in Fig. 6(d) show no obvious change trend. The annual average maximum of 2.78×10^6 km^2 occurred in 2016, while the maximum daily extent of 2.78×10^6 km^2 (24.8% of the total sea ice) occurred at September 29th, 2016, i.e. in the same year. The minimum daily extent of 0.74×10^6 km^2 occurred at March 1st 2017, but it accounts for a large proportion (36.1%) of the sea ice area.

5. Discussion

The concept of MIZ relies on several sea ice properties, such as ice concentration, ice thickness, ice floe sizes and shapes. Previous studies commonly selected a single property to determine the spatial extent of MIZ (Strong, 2012; Strong and Rigor, 2013; Stroeve et al., 2016; Liu et al., 2021). In this study, we attempted to integrate several properties to a single representative variable as a proxy of the MIZ, and used the FIS as a framework to realize this integration process. In our previous

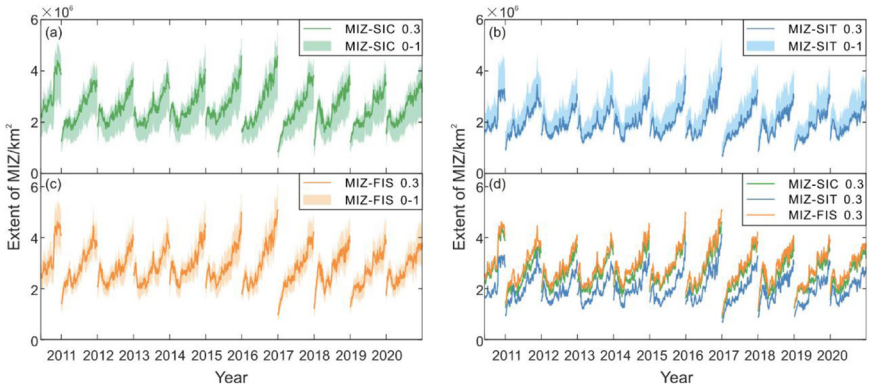

Fig. 6. Temporal change of Antarctic MIZ presented by (a) MIZ-SIC, (b) MIZ-SIT, (c) MIZ-FIS, of which the solid lines for the alpha-cut 0.3, and shaded areas for uncertain interval.

research, random sets were used to quantify the spatial–temporal uncertainty of Antarctic sea ice extent (Zhao et al., 2016), which though was applied to one variable — sea ice concentration, and not yet developed for multiple variables. In contrast, FIS can involve multiple variables by setting several fuzzy rules and is thus applicable for the complex concept-driven extraction.

When applying FIS we needed to set up membership functions, fuzzy rules and a defuzzification method. There are several ways of setting membership function, such as fuzzy methods (Zadeh, 1978), binary comparison ranking (Wang et al., 2014) and expert investigation. In this study, we proposed to use a gradient index for capturing the variability of SIC and SIT thresholds, and thus to determine the threshold scene by scene. In doing so we were able to construct membership functions reflecting the variability of the thresholds. These functions were therefore derived from the data themselves. In the final defuzzification step, we proposed a new method, i.e., the q-statistic (Wang et al., 2016), to find the optimal alpha-cut for defuzzification. The q-statistic was designed to measure the degree of spatial partition and to test its significance. A q value is in the interval [0,1]; a large q value corresponds with a better spatial partition. The optimal alpha-cut would give us a strong hard classification result that has less within-class variation than between-class variation. Calculating the q value for FIS membership from 0.1,0.2, 0.3, …, 1, we found that the membership 0.3 with the largest q value as alpha-cut was optimal for conducting defuzzification.

SIT data were incomplete in the summer period, while the accuracy of SIC data reduced during the melting season. Possibly, other data source like SAR could be used to make a more complete time series of SIT and SIC, and consequently a complete series of MIZ. This kind of MIZ data is likely to be valuable for polar climate change research. After our previous spatial analyses of the Antarctic sea ice extent (Zhao et al., 2016; Liu et al., 2021), the current study also addressed the Antarctic MIZ to demonstrate our concept-driven extraction method. Similar processes can be done for the Arctic MIZ, where sea ice experiences more rapid changes, i.e., less coverage and thickness, younger and more mobile (Kwok, 2018). Based upon complete and accurate MIZ information, we can then make a further step to explore feedback of MIZ on the whole polar climate system.

Our study shows that fuzzy modeling serves as a welcome addition to spatial statistics and can have an impact in climate change studies. We used fuzzy modeling as a complimentary methodology to random sets modeling in a dynamic setting for identifying changes in sea ice concentrations and related variables, including their uncertainties. Most if not all climate change variables have a spatial–temporal signature and these require a skillful and well targeted analysis. The methodology as presented in this paper can be extended to an arbitrary number of variables in a straightforward way. Fuzzy methods, originating from computer science, are not new in statistics (see Manton et al. (1994)), but a further integration to spatial and spatio-temporal statistical will be a challenge for the future.

6. Conclusions

The marginal ice zone (MIZ) is a human defined concept, which has a direct and sharp relation with a target on the earth surface. To extract the MIZ extent from a series of images, we need to derive it from several sources, which also involves quantification of uncertainties in its definition, the individual data and thresholding. In this study, we presented a fuzzy inference system (FIS) to integrate two characteristics: sea ice concentration (SIC) and sea ice thickness (SIT). Fuzzy membership functions were used to quantify the distribution of SIC and SIT with multi-thresholds and to estimate the spatial uncertainty of the MIZ extent. Results showed that the MIZ-FIS successfully integrated more than one dataset to provide a comprehensive identification. The indeterminate part of MIZ was presented by the support set, which delineates the natural variation of MIZ boundary. This method is applicable if more properties and input datasets are being involved.

Acknowledgments

This research is supported by Innovation Group Project of Southern Marine Science and Engineering Guangdong Laboratory (Zhuhai) (No. 311021008). We thank the reviewers and editor for their constructive comments, which contributed to the final paper.

References

Comiso, J.C., 2006. Abrupt decline in the Arctic winter sea ice cover. Geophys. Res. Lett. 33 (18), L18504.

Hong, T.P., Lee, C.Y., 1996. Induction of fuzzy rules and membership functions from training examples. Fuzzy Sets Syst. 84 (1), 33–47.

Huntemann, M., Heygster, G., Kaleschke, L., Krumpen, T., Mäkynen, M., Drusch, M., 2014. Empirical sea ice thickness retrieval during the freeze-up period from SMOS high incident angle observations. Cryosphere 8, 439–451. http://dx.doi.org/10.5194/tc-8-439-2014.

Kwok, R., 2018. Arctic sea ice thickness volume, and multiyear ice coverage: losses and coupled variability (1958-2018). Environ. Res. Lett. 13 (10), 105005. http://dx.doi.org/10.1088/1748-9326/aae3ec.

Lee, C.M., Cole, S., Doble, M., Lee, F., Hwang, P., Jayne, S., et al., 2012. Marginal Ice Zone (MIZ) Program: Science and Experiment Plan. Technical Report APL-UW 1201,, University of Washington.

Li, Y.M., Shi, Z.K., Li, Z.H., 2002. Approximation theory of fuzzy systems based upon genuine many-valued implications - siso cases. Fuzzy Sets and Systems 130 (2), 147–157.

Liu, Y., Pang, X.P., Zhao, X., Alfred, S., Xiang, Z., Qing, J., Meng, Q., Jiang, D., 2021. Prediction of the antarctic marginal ice zone extent based upon its multifractal property. Fractals 29 (2), 2150035.

Manton, K.G., Woodbury, M.A., Tolley, H.D., 1994. Statistical Applications using Fuzzy Sets. John Wiley and Sons, New York.

Parkinson, C.L., 2019. A 40-y record reveals gradual Antarctic sea ice increases followed by decreases at rates far exceeding the rates seen in the Arctic. Proceedings of the National Academy of Sciences 116 (29), 14414–14423.

Shokr, M., Sinha, N., 2015. Sea ice: Physics and remote sensing.

Squire, V.A., 2007. Of ocean waves and sea-ice revisited. Cold Reg. Sci. Technol. 49 (2), 110–133.

Stroeve, J.C., Jenouvrier, S., Campbell, G.G., Barbraud, C., Delord, K., 2016. Mapping and assessing variability in the antarctic marginal ice zone, pack ice and coastal polynyas in two sea ice algorithms with implications on breeding success of snow petrels. Cryosphere 10 (4), 1823–1843.

Strong, C., 2012. Atmospheric influence on Arctic marginal ice zone position and width in the Atlantic sector, february–1979–2010. Clim. Dyn. 39, 3091–3102. http://dx.doi.org/10.1007/s00382-012-1356-6.

Strong, C., Foster, D., Cherkaev, E., Eisenman, I., Golden, K.M., 2017. On the definition of marginal ice zone width. J. Atmos. Ocean. Technol. 34 (7), 1565–1584.

Strong, C., Rigor, I.G., 2013. Arctic marginal ice zone trending wider in summer and narrower in winter. Geophys. Res. Lett. 40 (18), 4864–4868.

Wang, W.C., Xu, D.M., Chau, K.W., Lei, G.J., 2014. Assessment of river water quality based on theory of variable fuzzy sets and fuzzy binary comparison method. Water Res. Manag. Int. J. 28 (12), 4183–4200.

Wang, J., Zhang, T., Fu, B., 2016. A measure of spatial stratified heterogeneity. Ecol. Indic. 67, 250–256.

Weeks, W.F., 2010. On Sea Ice. Fairbanks. University of Alaska Press, Alaska, p. 664.

Williams, R., Kelly, N., Boebel, O., et al., 2014. Counting whales in a challenging, changing environment. Sci. Rep. 4, 4170.

WMO sea-ice nomenclature, 2014. WMO/OMM/BMO 259, Suppl. Vol. 5, pp. 23.

Yuan, X.H., Liu, Z.L., Lee, E.S., 2011. Center-of-gravity fuzzy systems based on normal fuzzy implications. Comput. Math. Appl. 61 (9), 2879–2898.

Zadeh, L.A., 1975. The concept of a linguistic variable and its application to approximate reasoning—I. Inform. Sci. 8 (3), 199–251.

Zadeh, L.A., 1978. Fuzzy sets as a basis for a theory of possibility. Fuzzy Sets and Systems 1 (1), 3–28.

Zhang, S.G., Zhao, J.P., Li, M., Liu, S.X., Zhang, S.W., 2018. An improved dual-polarized ratio algorithm for sea ice concentration retrieval from passive microwave satellite data and inter-comparison with ASI, ABA and NT2. J. Oceanol. Limnol. 36 (005), 1494–1508.

Zhao, X., Xu, L., Stein, A., Pang, X.P., 2016. The impact of averaging methods on the trend analysis of the Antarctic sea ice extent and perimeter. Spat. Statist. 18(Part A) 22, 1–233.